06,10

Friction-induced polarization dynamics in $Bi_4Ti_3O_{12}$ thin films

© E.D. Mishina[1], V.R. Bilyk[2], N.E. Sherstyuk[1], V.M. Mukhortov[3], K.P. Sharanov[1,¶], M.B. Agranat[4], A.V. Ovchinnikov[4], A.S. Sigov[1]

[1] MIREA — Russian Technological University, Moscow, Russia
[2] Radboud University, Nijmegen, The Netherlands
[3] Southern Scientific Center, Russian Academy of Sciences, Rostov-on-Don, Russia
[4] Joint Institute for High Temperatures, Russian Academy of Sciences, Moscow, Russia

¶ E-mail: sharanov@mirea.ru

Received August 7, 2023
Revised September 27, 2023
Accepted October 24, 2023

The results of an experimental study by the method of terahertz pumping — nonlinear optical sensing of the picosecond dynamics of ferroelectric polarization induced by the action of a terahertz pulse in a ferroelectric film $Bi_4Ti_3O_{12}$ on a silicon substrate in a wide range of the electric field strength of a THz pulse are presented. Numerical modeling based on the Landau−Khalatnikov equation of the dependences of the intensity of the second optical harmonic on the electric field shows the presence of a threshold THz field with an amplitude of $E_{th} = 4.5$ MV/cm. It is shown that for small fields $E < E_{th}$, the polarization fluctuates within a certain minimum of the two-minimum potential, although in time the second harmonic signal follows the terahertz pulse. At $E > E_{th}$, polarization is switched and the time dependence of the intensity of the second harmonic becomes more complicated. Based on a comparison of theoretical and experimental data, the conditions for switching polarization by a strong electric field of a picosecond HZ pulse are analyzed.

Keywords: ultrafast dynamics, polarization switching, terahertz radiation, ferroelectric films, bismuth titanate, second harmonic generation.

DOI: 10.61011/PSS.2023.12.57692.174

1. Introduction

Terahertz radiation and the effects it induced have great potential for practical application both for the development of photonic and electronic devices of new generation, and for fundamental studies aimed at identifying new properties of known functional materials [1–3]. In particular, the advantage of using THz radiation for ferroelectrics is the possibility of electrodeless application of an electric field to the ferroelectric and, thus, influencing its polarization in the pico(femto)second time range.

For ultrashort time intervals, recording of changes caused by the electric field of a laser (THz) pulse is a rather complex task, which often cannot be solved by traditional electrophysical methods. In this case, time-resolved X-ray diffraction methods [4,5] and optical (nonlinear optical) methods [6,7] are used, which make it possible to detect a non-stationary shift of ions, leading to modulation of dielectric polarization. X-ray methods make it possible to obtain direct evidence of the ion sublattice shift in a crystal under the influence of the electric field of THz pulse. However, time-resolved X-ray diffraction is available mainly at synchrotron sources. The second harmonic generation (SHG) method provides a much less expensive, but very fast and informative method for studying polarization behavior, based on the general proportionality of the SH field to the ferroelectric polarization vector [8–11]. On the other hand, the dependence of the SHG intensity on the electric field can be of a purely electronic nature, for example, in semiconductors at low fields (SHG or EFISH induced by the electric field). Thus, direct evidence of ion motion is extremely important for the interpretation of SHG results.

Over the last decade, THz-induced effects have been studied in the most common ferroelectrics, both in model crystals ($SrTiO_3$ [12], $LiNbO_3$ [13], $BaTiO_3$ [7]), and in technological materials widely used in electronic devices (thin films $BaSrTiO_3$ [14,15], heterostructure $PbTiO_3/SrTiO_3$ [16], as well as various structures based on them (for example, in ferroelectric photonic crystals BST/PZT [17]). In similar experiments the electric field is oriented in the sample plane. This configuration is used for modulators, phase shifters, tunable filters, phased array antennas, sensors, and some types of memory elements. However, domain structures with a polarization vector lying in the film plane were understudied, despite the fact that they could potentially be useful in memory elements based on FeFET transistors, as well as in photonics devices, in which domains can be manipulated with vertical domain walls using optical radiation.

Bismuth titanate $Bi_4Ti_3O_{12}$(BiTO) is considered as one of the most promising materials for FeFET memory elements

in the metal — ferroelectric-semiconductor structure -due to high residual polarization and Curie temperature [18]. The polarization mechanism in BiTO is associated with the inclination of the octahedron TiO_6 in the latice cell relative to the axis c and the displacement of bismuth atoms along the axis a [19–21]. In this case, the spontaneous polarization along the axis a ($55\,\mu C/cm^2$) in BiTO films is significantly higher than along the axis c ($4\,\mu C/cm^2$). However, BiTO epitaxial films have a strong tendency to grow with a preferred orientation (001) (axis c) [22–24], and it is expected that they will demonstrate significant polarization when switching in planar geometry.

This paper presents experimental studies of the dynamics of the ferroelectric order parameter initiated by a powerful picosecond THz pulse in BiTO films. To prove the dynamic switching of dielectric polarization in the film under the action of THz pulse, the dependence of the SHG intensity on transition, as well as amplitude, values of the electric field within the THz pulse were studied and confirmed by computer modeling.

2. Description of samples

Bismuth titanate films 450 nm thick were deposited by RF sputtering of ceramic targets (unit „Plasma 50 SE“, substrate temperature 26xEC, oxygen pressure in the chamber 0.7 Torr) on ngle-crystalline silicon (100)Si substrates with an insulating sublayer $(Ba_{0.6}Sr_{0.4})TiO_3$ (BST) 4 nm thick. The BST use as an insulating sublayer reduces the lattice mismatch of the ferroelectric and the silicon substrate, which, in turn, prevents degradation of the polarization state at the interface [25,26], and improves the structural quality of the film.

The structural perfection of the sample, the lattice cell parameters, as well as the epitaxial relationships between the layers were measured at room temperature by X-ray diffraction (DRON-4-07, Cu K_α-radiation). As can be seen in Figure 1, $\Theta-2\Theta$ the diffraction pattern of the sample contains only (00L) peaks corresponding to BiTO. This indicates that (001) plane of the BiTO film is parallel to the substrate plane, the film is single-crystal, and the a and b axes are directed in the substrate plane. The vertical misorientation is approximately 4 degrees. The lattice parameters of the structure are $a = 0.5448$ nm, $b = 0.5411$ nm and $c = 3.289$ nm. The value of the lattice cell parameter normal to the substrate is higher than that of the bulk sample [27,28], which indicates the presence of two-dimensional stresses in the film in the plane of the substrate. Taking into account the X-ray diffraction data, we can state that the BiTO film contains a 180-degree domain structure in the film plane, which coincides with the results of the paper [29].

3. Experiment

Experimental studies of the THz-induced dynamics of ferroelectric polarization in Si/BST/BiTO structures were carried out using the THz pumping method — nonlinear optical probing in „reflection“ geometry [14]. THz pumping pulses were generated by the optical rectification method in a nonlinear optical crystal OH1. To increase the range of the applied terahertz electric field, two laser systems with a wavelength of 1240 nm and a pulse width of 100 fs were used („Avesta-Project“, Russia). The LS1 laser system provides the electric field amplitude of up to 1.3 MV/cm at a pulse repetition rate of 100 Hz and an energy per pulse about $2\,\mu$J. Further we will call the range of values obtained using LS1 as the range of „weak“ fields. On LS2 laser system the maximum amplitude of the electric field was up to 23 MV/cm (hereinafter —„strong“ fields) at a pulse repetition rate of 10 Hz and pulse energy $105\,\mu$J. All measurements were carried out in dry air with humidity less than 2% to exclude THz radiation absorption by water vapor.

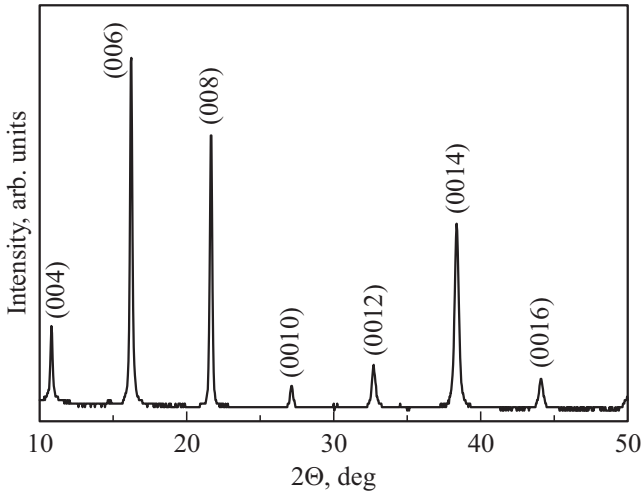

Figure 1. X-ray diffraction pattern of Si/BST/BiTO structure.

The time dependences of the electric component of the THz pulse field, measured by the electro-optical gating method using LS1 and LS2 units, are shown in Figure 2 (right scale). According to the Fourier spectra obtained for both time dependences (insert in Figure 2), the central generation frequency is 1.7 THz for the „weak“ field unit and 1.5 THz for the „strong“ field unit with spectral width (FWHM) about 1.23 and 1.5 THz, respectively.

To form a probe beam 10% of the IR radiation in each laser system was directed to the sample surface using a beam splitter and an automated delay line. The angle of incidence on the sample surface was 45 degrees. The SHG intensity, as a measure of ferroelectric polarization, was measured using a photomultiplier tube. Details of the registration technique can be found in paper [15]. Figure 2 shows the characteristic time dependences of the SH intensity measured for the LS1 and LS2 units (left scale). Measurements of the SH intensity before the moment of exposure to the THz pulse (region near -0.6 ps in Figure 2) showed that the signal magnitude does not exceed the noise level, which can be explained by the unpolarized initial state of the sample. Thus, the experimental curves presented are due only to the contribution of the THz-induced SH.

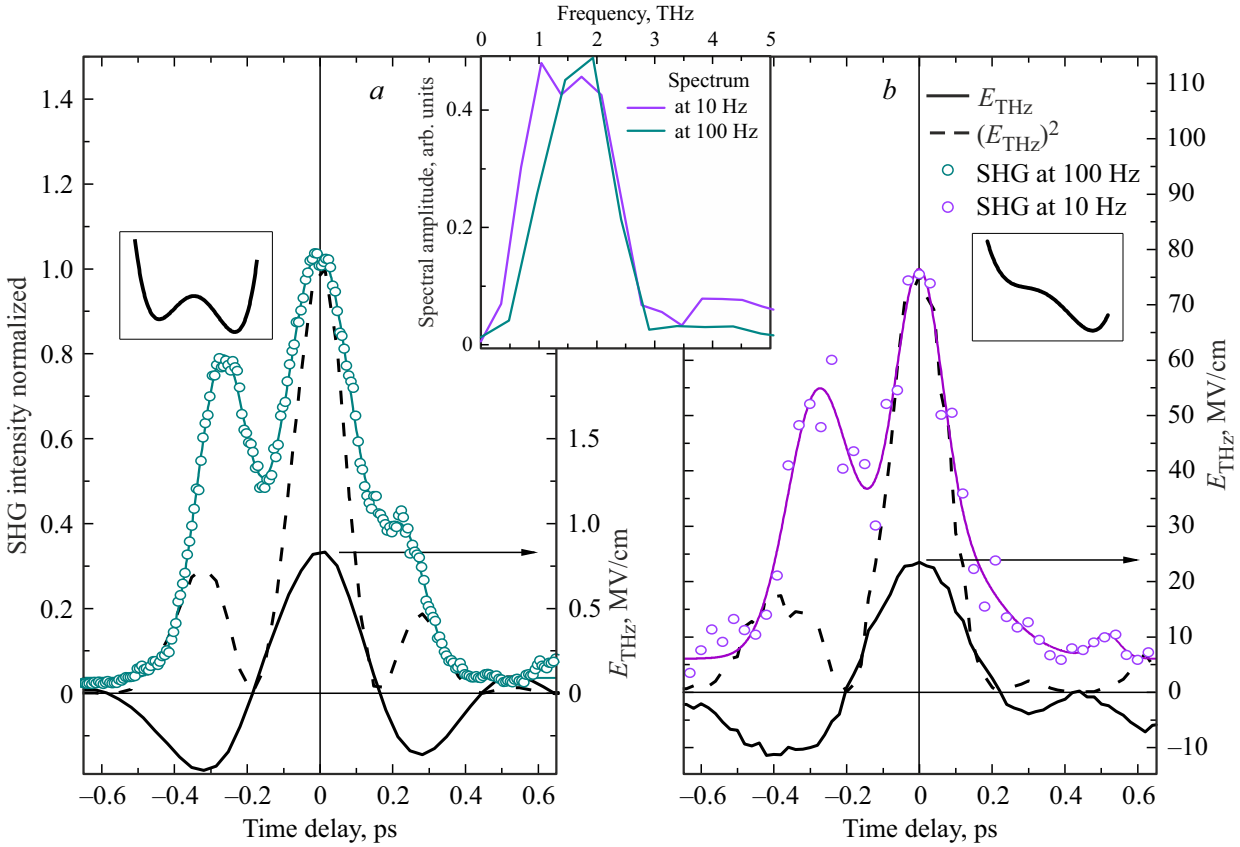

Figure 2. Time dependences of the electric field strength of a terahertz pulse $E_{\mathrm{THz}}(t)$and the square intensity $\left(E_{\mathrm{THz}}(t)\right)^2$, normalized to the maximum, and time dependences of SHG intensity (dots refer to the experiment, thin solid lines — markers for the eyes) for laser sources with a pulse repetition rate: (*a*) 100 Hz („weak" fields), (*b*) 10 Hz („strong" fields). The Figures show the corresponding forms of the double-well potential. Outside the specified time range, the magnitude of SH signal does not exceed the noise level. Insert: Fourier spectra of the corresponding THz pulses.

Since the SH intensity shall be proportional to the square ferroelectric polarization, which, in turn, depends on the electric field $E_{\mathrm{THz}}(t)$ of THz pulse, Figure 2 also shows the time dependences $\left(E_{\mathrm{THz}}(t)\right)^2$. Qualitatively, the SH intensity $I^{\mathrm{SHG}}(t)$ repeats the form of the dependence $\left(E_{\mathrm{THz}}(t)\right)^2$.

4. Results and discussion

The source of SHG in a ferroelectric film is dielectric polarization P_{THz}induced by the action of THz field

$$I^{(2\omega)} \propto (P_{\mathrm{THz}})^2 = \left(P(E_{\mathrm{THz}})\right)^2. \qquad (1)$$

In accordance with the Landau–Khalatnikov equation [31,32], the time dependence of the THz-induced polarization can be represented in the form

$$\mu \frac{d^2\mathbf{P}(t)}{dt^2} + \gamma \frac{d\mathbf{P}(t)}{dt} + \alpha_1 \mathbf{P}(t) + \alpha_{11}\mathbf{P}^3(t) + \alpha_{111}\mathbf{P}^5(t) = E_{\mathrm{THz}}(t). \qquad (2)$$

The phenomenological constants in equation (2) unambiguously characterize the shape of the double-well potential and the equilibrium states of polarization at fixed temperature T. Since the measurements were carried out at room temperature, the values of the phenomenological constants for BiTO were taken to be equal to those in paper [33]: $\alpha_1 = \alpha_T(T - T_c)$, $\alpha_T = 0.25 \cdot 10^6$, $T_c = 948$ K, $\alpha_{11} = -0.8586 \cdot 10^9$ and $\alpha_{111} = 6.9 \cdot 10^9$. Position of minimums calculated for the selected parameters are $|\mathbf{r}| = 5.7$ pm. The parameters $\mu$and γin equation (2) are the kinetic constants and damping constants, respectively, and are adjustable parameters that are chosen according to the best agreement with the experimental results.

In the calculations, it was assumed that the electric field $\mathbf{E}_{\mathrm{THz}}$ and the lateral (in the sample plane) polarization component are directed along the axis X of the laboratory coordinate system, therefore equation (2) was considered as one-dimensional problem, for the solution of which the Landau–Khalatnikov equations were written for each pair of lattice cells with the initial polar positions of the ions $x_0 = \pm 5.7$ pm. Further, the dynamic response of the SH intensity can be represented as $I^{(2\omega)} \propto (P_{+x} + P_{-x})^2$, where $P_{\pm x}$ — solutions to equation (2) obtained for two boundary conditions. This dependence, where the algebraic sum of polarizations is essentially the difference in responses

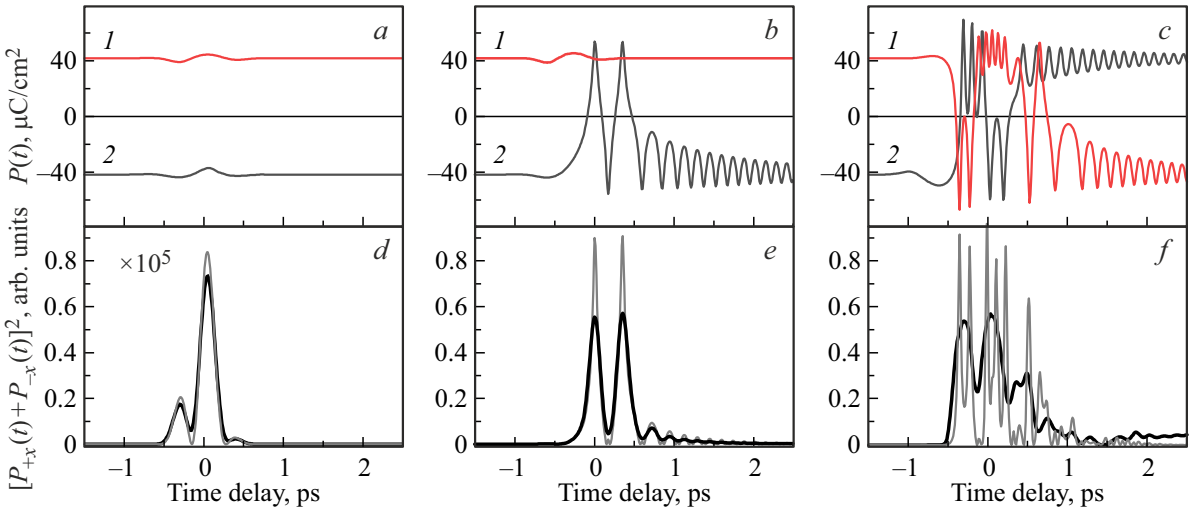

Figure 3. (*a–c*): Time dependences of THz-induced polarization calculated on the basis of formula (2) for „weak“ and „strong“ THz pulse fields with amplitude: $E_{\mathrm{THz}} = 0.5$ MV/cm (*a*); 5.3 MV/cm (*b*); 22 MV/cm (*c*). Curves *1* and *2* refer to different initial polar positions of the ions. (*d–f*) Time dependences of the square sum of polarizations obtained on the basis of the upper panels for each value of THz field (thin lines) and the result obtained by convolution using the formula (3) of the time forms of square polarization and the probe pulse (bold lines).

arising at opposite offsets, leads to the fact that the time dependences of the SH signal shown in Figure 2 are less „extended“ in time than the square intensity of THz fields. Figure 3 shows the time dependences of THz-induced polarization calculated on the basis of formula (2) for „weak“ and „strong“ terahertz fields.

Within the framework of the proposed model based on the double-well potential, the initial state of the ferroelectric is depolarized, i. e., the contributions of ions located in different polar positions ($P_{\pm x} = \pm 42\,\mu$C/cm^2) are equal. To switch polarization, it is required that the external field strength exceed a certain threshold value E_{th}, sufficient to overcome the potential barrier between the minima. For the potential given by equation (2), taking into account the above values of the phenomenological constants, the threshold value of field is $E_{\mathrm{th}} = 4.5$ MV/cm. In the area of fields lower than E_{th}, polarization switching does not occur, and the dipole moment fluctuates around its equilibrium value (Figure 3, *a*). Since such motion in the field of the terahertz pulse is coherent, it leads to polarization modulation (Figure 3, *d*).

As the magnitude of the exciting field approaches the critical, the states of the ions occupying opposite minima in the double-well potential become nonequivalent with respect to the external field. If the external field is directed in such a way that the ions offset caused by it occurs in the direction of the potential barrier, then for a given group of ions a transition to the opposite minimum occurs, i. e., switching. The same effect for a group of ions in the opposite state does not cause switching. Thus, different vibrational behavior is observed near the equilibrium position of ions with opposite initial positions (Figure 3, *b*). With a further field increasing the ions from both positions of the minimum overcome the potential barrier and, having oscillated with a transition from minimum to minimum, can find themselves in positions opposite to the initial ones (Figure 3, *c*). In this paper the simulation results are presented only for two cells with opposite initial ion positions, i. e., for a single combination of initial and boundary conditions. It is obvious that, taking into account thermal motion, the initial positions of the ions and their initial velocities will differ also. Averaging over various combinations of initial and boundary conditions will lead to „blurring“ of the time shape of the SH signal.

Thus, calculations show that only starting from a some value of the THz field E_{th} the ion jump into the adjacent potential well is possible. At lower fields, however, a coherent offset of ions occurs in the direction of the THz pulse field, which causes polarization modulation. Based on the type of experimental dependences of the SH intensity, it is impossible to distinguish between the modulation region without dynamic switching and the region where such switching (ion jump to the neighboring minimum) occurs.

The square total polarization, which determines the intensity of the second harmonic, is presented in Figure 3, *d–f* (thin lines). It is obvious that the curves obtained in this way for the case of high fields do not coincide (Figure 3, *f*) with the experimental curves shown in Figure 2. For a correct comparison it is necessary to take into account the duration of the probing pulse, i. e. to perform a time convolution of this pulse with the pulse of the generated SH. Then the experimental time dependence of SH intensity will have the form

$$I^{2\omega}(t) \propto \left(\int_0^{\tau_{\mathrm{THz}}} \left(P_{+x}(t-\tau)+P_{-x}(t-\tau)\right) E^{\omega}(\tau) E^{\omega}(\tau)\, d\tau \right)^2. \tag{3}$$

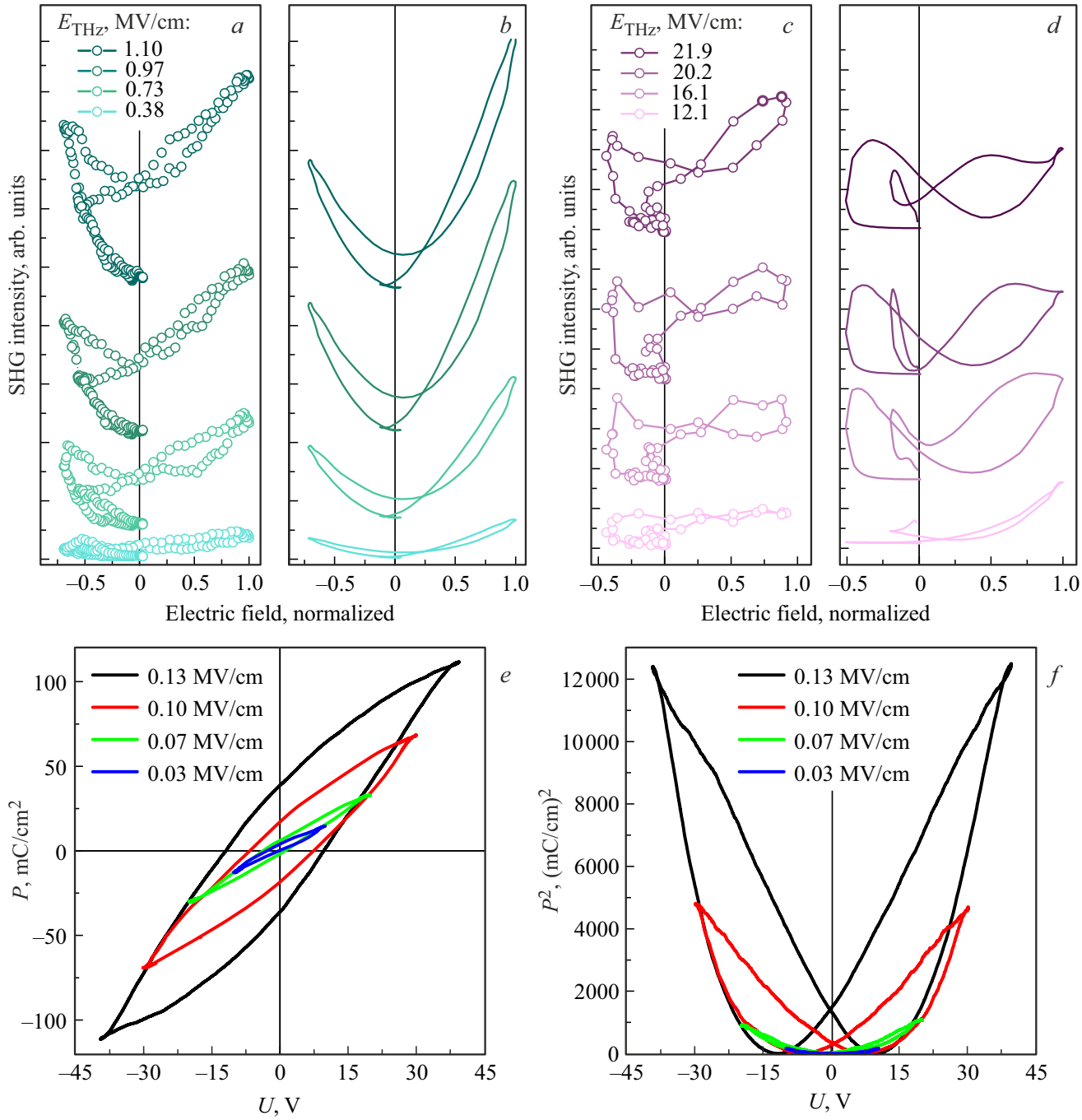

Figure 4. (a–d) SHG hysteresis loops $I^{2\omega}(E_{THz})$ for different values of the electric field strength of the THz pulse for „weak“ (a, b) and „strong“ (d, c) fields; (a, c) — experiment, (b, d) — calculation in accordance with equations (2) and (3) with $\mu = 2 \cdot 10^{-19}$ Jm/A^2, $\gamma = 10^{-7}$ Jm/A$^2 \cdot$ s. The starting point for the measurement corresponds to $I^{2\omega} = 0$. The curves are shifted relative to each other vertically for clarity. (e) Dielectric hysteresis of MgO/BST/BiTO structure (450 nm), measured in planar geometry of electrodes at an external voltage frequency of 32 Hz at various electric field amplitudes. (f) Corresponding dependence of the square dielectric polarization on the external voltage.

The dependence obtained in this way for $E_{THz} = 22$ MV/cm, presented in Figure 3, f (thick line), qualitatively coincides with the dependences observed in the experiment (Figure 2). For field values $E_{THz} = 0.5$ MV/cm and $E_{THz} = 5.3$ MV/cm, convolution does not change the shape of the curve.

Independent measurements of the electric field of THz pulse and the SHG response make it possible to parametrically obtain SHG hysteresis, which is actually the hysteresis of the square polarization. This can be done both from experimental data and from simulation results. The corresponding curves demonstrating the change in dynamic

hysteresis loops with increasing field strength of the THz pulse are shown in Figure 4, *a*–*d*.

Over the entire range of fields studied, the dynamic SHG hysteresis are nonlinear, and the dependence $I^{2\omega}(E_{\mathrm{THz}})$ is quadratic. In this case, the response to the influence of fields with opposite signs significantly differs: in addition to the amplitudes difference, in the region of negative fields the SH hysteresis loops have a characteristic distortion (lateral bending).

To assess the effectiveness of the field influence of THz pulse on the state of polarization in the BiTO ferroelectric film, we compared the obtained SHG loops with low-frequency (32 Hz) dielectric polarization hysteresis measured in planar geometry of electrode at different external field values by the Sawyer–Tower method [29] in similar structures on MgO substrate (Figure 4, *e*). Despite the different properties of the substrates, such comparison is acceptable, since during electrical measurements the semiconductor substrate is involved in the processes of charge redistribution in the structure when the external field is applied (for example, due to the formation of enriched/depleted region of main carriers in the near-surface layer of silicon [24], Schottky barrier, etc.), while the dielectric MgO substrate has practically no effect on polarization switching at the same ferroelectric thickness.

For electrophysical measurements the planar electrodes with interdigital transducer structure and a gap between the electrodes 3 μm were deposited on the surface of the BiTO film in MgO/BST/BiTO structure. The electric field generated using this structure in the gap between the electrodes when applying a voltage with amplitude $U = \pm 40$ V does not exceed 0.13 MV/cm, i. e. to obtain fields comparable to terahertz fields, it is necessary to use significantly higher voltage. It can be noted that for the electrophysical dependences there is also a threshold value below which the residual polarization is close to zero (Figure 4, *e*), i. e. external voltage does not switch the ferroelectric film between two stable states, and the dependence $[P(U)]^2$ has the shape of a parabola (Figure 4, *f*). Above the critical value, a pronounced hysteresis of the dependence $P(U)$ with residual polarization value $P_r(U = 40\,\mathrm{V}) = 38\,\mu\mathrm{C/cm}^2$ is observed.

The intensity of SHG signal depending on the magnitude of THz field at the maxima of the time dependence (see Figure 2) is shown in Figure 5. The „weak" fields mode obtained from simulations in the range from −5 to 5 MV/cm corresponds to the non-switching case where the polarization modulation, described by the quadratic term of the free energy density and the polar ion, occurs in harmonic potential. In the given range of terahertz electric fields, the curves of the experimental and calculated results coincide (insert in Figure 5). In the region of „strong" fields (10–20MV/cm), a noticeable discrepancy between the experimental data and the simulation results is observed.

Both dependencies are described by a power function with a quadratic term $I^{(2\omega)} \propto (\chi^{(3)}E_{\mathrm{THz}})^2$. Above the field ~ 5 MV/cm („strong" fields), the behavior of the structure

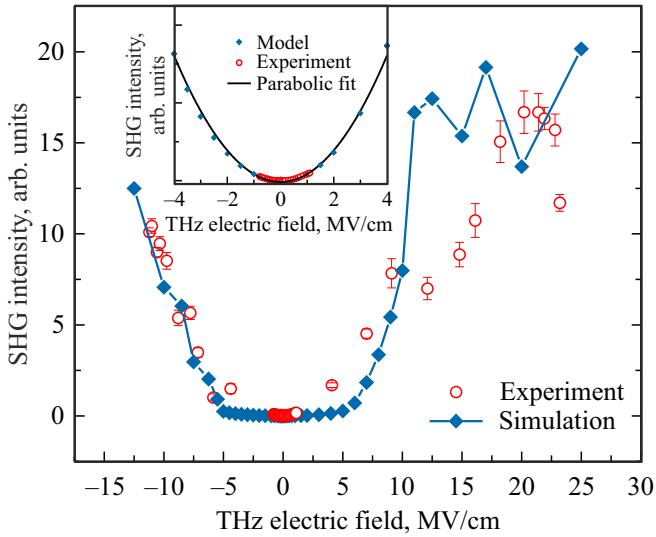

Figure 5. Experimental (open symbols) and calculated (closed symbols) SHG intensity vs. electric field of THz pulse in the region of „strong" fields. In insert: comparison of experimental and calculated results for „weak" fields in the region ±1 MV/cm.

corresponds to dynamic switching, accompanied by a sharp increase in SHG intensity. This behavior is described in terms of the ions movement when polar ion passes the potential barrier to the opposite minima of the double-well potential [14]. At field value about 18 MV/cm, the SH intensity reaches saturation within the measurement error. The saturation region is small, since with further increase in the field, a decrease in the signal is observed due to the sample heating.

5. Conclusion

The results of the action of powerful THz pulse on thin ferroelectric films $Bi_4Ti_3O_{12}$, obtained by the method of THz pumping — nonlinear optical probing, show that this effect leads only to a dynamic switching of polarization, i. e. after the end of THz-pulse action the system returns to its initial state.

The dynamic response of SHG intensity, obtained as a result of solving the Landau–Khalatnikov equation, for the entire set of initial states and field strengths of the exciting THz pulse is proportional to the square total polarization $I^{(2\omega)} \propto \sum_i (P_i)^2$. Qualitatively, the calculated dependences of SH intensity for various pumping field strengths have the form of the square field strength of THz pulse and are identical in nature to the experimental results. This type of dependence appears when the SHG response from unperturbed sample is relatively low compared to the signal induced by THz radiation, and there is no contribution from the interference term to the SHG intensity.

Despite the fact that the experimental results did not reveal a stable switching to one of the stable states, nevertheless, theoretical calculations show that such switching is

possible when certain experimental conditions are reached, which are currently not realized. Factors influencing the dynamic nonlinear optical response include, first of all, the strength of the THz pulse.

Funding

This study was supported by the Russian Science Foundation, grant No. 22-12-00334. The experiment was carried out on a unique scientific set-up „Laser terawatt femtosecond complex (LTFC)“, Joint Institute for High Temperatures RAN (JIHT RAN).

Conflict of interest

The authors declare that they have no conflict of interest.

References

[1] Y. Zhou, Y. Huang, X. Xu, Z. Fan, J.B. Khurgin, Q. Xiong. Appl. Phys. Rev. **7**, 041313 (2020).
[2] D.S. Rana, M. Tonouchi. Adv. Opt. Mater. **8**, 1900892 (2020).
[3] M.A. Kik, G.D. Bogomolov, A.S. Sigov, A.A. Shilyaev, V.V. Zavyalov, S.S. Verbitsky, A.N. Tselebrovsky. Ros. Tekhnol. Zhurn., **7**, 122 (2020). (in Russian).
[4] M. Kozina, M. Pancaldi, C. Bernhard, T. van Driel, J.M. Glownia, P. Marsik, M. Radovic, C.A.F. Vaz, D. Zhu, U. Staub, M.C. Hoffmann. Appl. Phys. Lett. **110**, *8*, 081106 (2017).
[5] M. Kozina, T. van Driel, M. Chollet, T. Sato, J.M. Glownia, S. Wandel, M. Radovic, U. Staub, M.C. Hoffmann. Struct. Dyn. **4**, *5*, 054301 (2017).
[6] T. Miyamoto, H. Yada, H. Yamakawa, H. Okamoto. Nature Commun. **4**, 2586 (2013).
[7] F. Chen, Y. Zhu, S. Liu, Y. Qi, H.Y. Hwang, N.C. Brandt, J. Lu, F. Quirin, H. Enquist, P. Zalden, T. Hu, J. Goodfellow, M.-J. Sher, M.C. Hoffmann, D. Zhu, H. Lemke, J. Glownia, M. Chollet, A.R. Damodaran, J. Park, Z. Cai, I.W. Jung, M.J. Highland, D.A. Walko, J.W. Freeland, P.G. Evans, A. Vailionis, J. Larsson, K.A. Nelson, A.M. Rappe, K. Sokolowski-Tinten, L.W. Martin, H. Wen, A.M. Lindenberg. Phys. Rev. B **94**, 180104 (2016).
[8] G. Dolino, J. Lajzerowicz, M. Vallade. Phys. Rev. B **2**, 2194 (1970).
[9] O.A. Aktsipetrov, A.A. Fedyanin, D.A. Klimkin, A.A. Nikulin, E.D. Mishina, A.S. Sigov, K.A. Vorotilov, M.A.C. Devillers, Th. Rasing. Ferroelectrics **190**, 143 (1997).
[10] M. Fiebig,, T. Lottermoser, D. Fröhlich, A.V. Goltsev, R.V. Pisarev. Nature **419**, 818 (2002).
[11] K.A. Grishunin, N.A. Ilyin, N.E. Sherstyuk, E.D. Mishina, A. Kimel, V.M. Mukhortov, A.V. Ovchinnikov, O.V. Chefonov, M.B. Agranat. Sci. Rep. **7**, 687 (2017).
[12] X. Li, T. Qiu, J. Zhang, E. Baldini, J. Lu, A.M. Rappe, K.A. Nelson. Science, **364**, 1079 (2019).
[13] R. Mankowsky, A. von Hoegen, M. Först, A. Cavalleri. Phys. Rev. Lett. **118**, 197601 (2017).
[14] V. Bilyk, N. Ilyin, E. Mishina, A. Ovchinnikov, O. Chefonov, V. Mukhortov. Scr. Mater. **214**, 114687 (2022).
[15] K. Grishunin, V. Bilyk, N. Sherstyuk, V. Mukhortov, A. Ovchinnikov, O. Chefonov, M. Agranat, E. Mishina, A.V. Kimel. Sci. Rep. **9**, *1*, 697 (2019).
[16] J. Ji, S. Zhou, J. Zhang, F. Ling, J. Yao. Sci. Rep. **8**, 2682 (2018).
[17] Y. Zeng, W. Wang, F. Ling, J. Yao. Photon. Res. **8**, *6*, 1002 (2020).
[18] A.S. Anokhin, S.V. Biryukov, Yu.I. Golovko, V.M. Mukhortov. FTT **61**, 278 (2019). (in Russian).
[19] D. Urushihara, M. Komabuchi, N. Ishizawa, M. Iwata, K. Fukuda, T. Asaka. J. Appl. Phys. **120**, 142117 (2016).
[20] S.H. Shah, P.D. Bristowe. J. Phys. Condens. Matter **22**, 385902 (2010).
[21] Yu Chen, J. Xu, Sh. Xie, Zh. Tan, R. Nie, Zh. Guan, Q. Wang, J. Zhu. Materials (Basel). **11**, 821 (2018).
[22] R. Ramesh, K. Luther, B. Wilkens, D.L. Hart, E. Wang, J.M. Tarascon, A. Inam, X.D. Wu, T. Venkatesan. Appl. Phys. Lett. **57**, 1505 (1990).
[23] Z. Cheng, C.V. Kannan, K. Ozawa, H. Kimura, X. Wang. Appl. Phys. Lett. **89**, 032901 (2006).
[24] A.S. Anokhin, Yu.I. Golovko, V.M. Mukhortov, D.V. Stryukov. FTT **61**, *11*, 2178 (2019). (in Russian).
[25] S.-H. Baek, C.-B. Eom. Acta Mater. **61**, 2734 (2013).
[26] Z. Yu, J. Ramdani, J.A. Curless, C.D. Overgaard, J.M. Finder, R. Droopad, K.W. Eisenbeiser, J.A. Hallmark, W.J. Ooms, V.S. Kaushik. J. Vac. Sci. Technol. B **18**, 2139 (2000).
[27] L.G. Van Uitert, L. Egerton. J. Appl. Phys. **32**, 959 (1961).
[28] R. Ramesh, K. Luther, B. Wilkens, D.L. Hart, E. Wang, J.M. Tarascon, A. Inam, X.D. Wu, T. Venkatesan. Appl. Phys. Lett. **57**, 1505 (1990).
[29] V.M. Mukhortov, D.V. Stryukov, S.V. Biryukov, Yu.I. Golovko. ZhTF **90**, *1*, 128 (2020). (in Russian).
[30] P.C.M. Planken, H.-K. Nienhuys, H.J. Bakker, T. Wenckebach. J. Opt. Soc. Am. B **18**, 313 (2001).
[31] J.-G. Caputo, E.V. Kazantseva, A.I. Maimistov. Phys. Rev. B **75**, 014113 (2007).
[32] V. Bilyk, E. Mishina, N. Sherstyuk, A. Bush, A. Ovchinnikov, M. Agranat. Phys. Status Solidi RRL **15**, 2000460 (2021).
[33] L.E. Cross, R.C. Pohanka. Mater. Res. Bull. **6**, 939 (1971).

Translated by I.Mazurov